Saturn: Search for a missing water source

S. Jurac,[1] M. A. McGrath,[2] R. E. Johnson,[3] J. D. Richardson,[1] V. M. Vasyliūnas,[4] and A. Eviatar[5]

Received 10 July 2002; revised 19 September 2002; accepted 27 September 2002; published 21 December 2002.

[1] The origin of the large hydroxyl radical (OH) cloud near the inner moons of Saturn, indicative of a surprisingly large water-vapor source, has represented a puzzle since its discovery in 1992. A new set of Hubble Space Telescope measurements is used to constrain the OH spatial densities and to pinpoint the source region. Our model indicates that the vast majority of the water vapor (>80%) originates from Enceladus's orbital distance. This may indicate the presence of a dense population of small, as of yet unseen, bodies concentrated near Enceladus; collisions between these fragments are the suggested mechanism for producing the necessary amounts of water vapor. We show that collisions between plasma ions and neutral molecules substantially inflate the OH cloud, and increase the OH loss rate, requiring a water source three times larger than previous estimates. *INDEX TERMS:* 6275 Planetology: Solar System Objects: Saturn; 2756 Magnetospheric Physics: Planetary magnetospheres (5443, 5737, 6030); 6280 Planetology: Solar System Objects: Saturnian satellites; 6213 Planetology: Solar System Objects: Dust. **Citation:** Jurac, S., M. A. McGrath, R. E. Johnson, J. D. Richardson, V. M. Vasyliūnas, and A. Eviatar, Saturn: Search for a missing water source, *Geophys. Res. Lett.*, *29*(24), 2172, doi:10.1029/2002GL015855, 2002.

1. Introduction

[2] The discovery of a dense toroidal OH atmosphere at Saturn [*Shemansky et al.*, 1993] presented a challenge to space physicists [*Johnson*, 1993]. This doughnut shaped cloud consists of water-group neutrals (H_2O, OH, O, H, O_2, H_2) that orbit the planet until they collide with and are absorbed by rings/moons, escape from Saturn, or are ionized forming the local plasma (O^+, OH^+, H_2O^+, H^+, e^-). Water molecules originating from the rings and/or moons presumably serve as the precursor molecules for these neutrals and plasma. The neutral number density is about ten times the plasma density [*Richardson*, 1998], so unlike Jupiter's magnetosphere, Saturn's is dominated by neutrals. It was suggested that a significant neutral population might evolve from the icy main rings [*Pospieszalska and Johnson*, 1991], which extend to 2.27 R_S. But the peak OH densities were found much further out, between the orbits of Enceladus (3.95 R_S) and Tethys (4.89 R_S), suggesting the source is in that region [*Richardson et al.*, 1998]. Since the net surface area of these moons is small, this raises an intriguing question: what is the source and the production mechanism for this water cloud?

[3] Sputtering, the process in which energetic plasma ions bombard the icy moons and ring particles ejecting water molecules from their surfaces, was shown to produce only a fraction of the water needed [*Johnson et al.*, 1989; *Jurac et al.*, 2001a]. Impacts on the moons and rings by micrometeorites, the small debris from asteroids and comets, also produce water vapor. Although interplanetary micrometeorite fluxes are uncertain, micrometeorite bombardment would produce peak densities close to the larger satellites and, especially, near the main rings [*Pospieszalska and Johnson*, 1991].

[4] A self-sustaining mechanism was proposed by *Hamilton and Burns* [1993]: they suggested that the E-ring, a diffuse tenuous ring with peak density at Enceladus, regenerates itself and produces the water vapor as part of this process [*Hamilton and Burns*, 1994]. Unlike Saturn's main rings, which contain centimeter to greater than meter-size objects, the E-ring is composed of tiny grains with diameters ranging from 0.3–3 microns [*Nicholson et al.*, 1996]. The E-ring grains become charged [*Jurac et al.*, 1995] and, due to their small mass, are easily influenced by the Lorentz and other forces [*Horanyi et al.*, 1992; *Dikarev*, 1999]. Hamilton and Burns suggested that these forces insert grains on highly eccentric orbits, subsequently resulting in high-speed grain-moon collisions. Such collisions would produce both water vapor and the fresh grains needed to replenish the E-ring.

[5] Finally, a large amount of debris residing near Enceladus, possibly remnants of a former moon that was broken apart, was suggested as a source. Orbital collisions among these fragments would produce the abundance of small grains necessary to replenish the E-ring and sputtering of these grains would provide water vapor [*Jurac et al.*, 2001b]. A bright arc disappearing in a matter of hours was recently observed near Enceladus, and was attributed to such a collision [*Roddier et al.*, 1998].

2. Observations

[6] The OH molecule efficiently scatters solar ultraviolet light at 3085 angstroms, thus OH is the water-group neutral most readily detected near Saturn. The Hubble Space Telescope (HST) Faint Object Spectrograph (FOS) observes the total OH content along a line-of-sight through the magnetosphere. Using many line-of-sight observations one can build a 3-D picture of the cloud's morphology. Nine such measurements have been previously published [*Shemansky et al.*, 1993; *Hall et al.*, 1996; *Richardson et al.*, 1998] and here we present an additional 8 measurements. These new measurements provide critical data at distances closer to Saturn and away from the equatorial plane.

[1]M.I.T., Cambridge, Massachusetts, USA.
[2]Space Telescope Science Institute, Baltimore, Maryland, USA.
[3]University of Virginia, Charlottesville, Virginia, USA.
[4]Max-Planck-Institut für Aeronomie, Katlenburg-Lindau, Germany.
[5]Tel Aviv University, Ramat Aviv, Israel.

0094-8276/02/2002GL015855$05.00

[7] Measurements of fluorescent OH emissions were obtained in 1996 from radial distances of 3 and 4.5 R_S from Saturn (HST FOS program 6755, PI: D. Shemansky) on the dusk side of the planet. The instrument's image mode provided readouts at two or three different y-deflections of the detector within the 4.3″ aperture, with each y-deflection corresponding to a different distance above or below Saturn's equatorial plane. Table 1 shows the observations and derived OH brightness values. The measured brightness values at 3 R_S are twice as large as the maximum brightness of 130 Rayleighs at 4.5 R_S found earlier. Thus the total OH content is larger than previously inferred, and the peak density (and thus, the source region) is between 3 and 4.5 R_S rather than between 4 and 5 R_S as previously reported [*Richardson et al.*, 1998].

3. Model

[8] The model developed to simulate the morphology of the cloud follows particles as they orbit in Saturn's gravitational field, from their injection until they are lost by ionization, by collisions with rings, moons, or Saturn, or by escape from the Saturnian system [*Jurac et al.*, 2001b]. Our model includes the effects of chemistry, neutral-neutral and plasma-neutral collisions, tracking the dynamical evolution of the water group neutrals in Saturn's magnetosphere. The dominant neutral dissociation channels: H_2O –> OH+H, H_2O –> O+H_2, OH –> O+H and their energy balances are considered. The lifetimes of the neutrals against loss to charge exchange, dissociative recombination and electron impact dissociation depend on local plasma energies and densities. Neutral lifetimes are based on a 2-D model [*Richardson et al.*, 1998] and include the effect of solar photodissociation. The total lifetimes are shortest in the equatorial plane where the plasma density peaks, ranging from 3 days (O) to almost 3 months (OH).

[9] The source rates of water molecules ejected from each moon are free parameters in the model and adjusted to give the best fit to the observations. The ejected neutrals, like the moons, orbit with speeds close to the local Keplerian speed, while the plasma ions are 'frozen-in' to the magnetic field and rotate with Saturn's spin rate. This velocity difference between fast ions and slower neutrals results in charge exchange and also in collisions in which momentum is transferred to the neutrals, expanding the cloud and causing the loss of neutrals. A Monte Carlo transport simulation

Table 1. Date of Observation, Time (UT), Distance From the Spin Axis R (R_S), Distance From the Equatorial Plane Z (R_S), and Measured Brightness (Rayleighs) With One-Standard-Deviation Level Uncertainties

Date	Time	R	Z	Brightness
Oct 04	20:09–23:48	3.0	−0.125	248 ± 50
Oct 04	20:09–23:48	3.0	0.000	324 ± 33
Oct 04	20:09–23:48	3.0	0.125	282 ± 33
Oct 12	10:24–14:57	4.5	−0.125	109 ± 7
Oct 12	10:24–14:57	4.5	0.000	122 ± 7
Oct 12	10:24–14:57	4.5	0.125	102 ± 7
Oct 12	15:06–21:43	4.5	0.254	98 ± 9
Oct 12	15:06–21:43	4.5	0.375	77 ± 7

The data have been reduced in the same manner as previous measurements [*Richardson et al.*, 1998; *Hall et al.*, 1996] and the brightness is normalized to a Saturn–Earth distance of 8.9 AU.

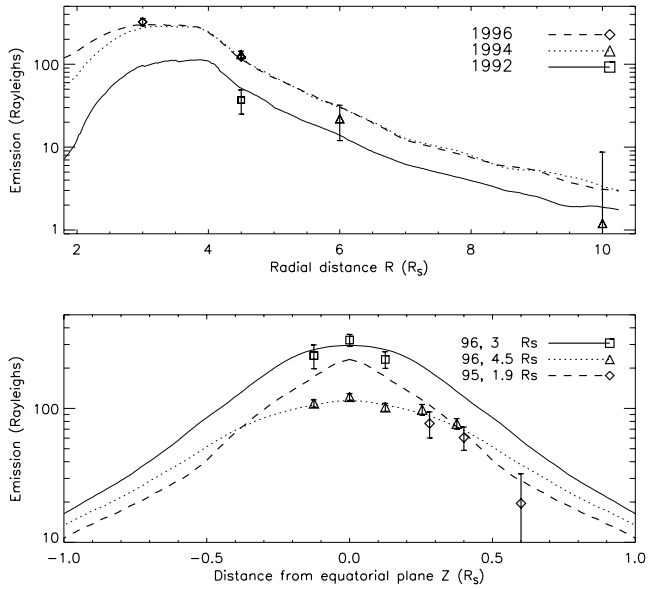

Figure 1. (a) Brightnesses profile of the OH cloud. Symbols represent inferred brightnesses from HST observations at the distances from Saturn as indicated, while lines represent modeled OH emission. (b) Same as (a) for vertical distance from the equatorial plane.

with 'ZBL' collisional potentials [*Eckstein*, 1991] was employed to describe ion-neutral and neutral-neutral collisions. The mean free path between collisions, as well as the distance of the closest approach between molecules, depends critically on ion and neutral densities. Ion densities were based on the Richardson and Sittler 2-D plasma model [*Richardson and Sittler*, 1990], while neutral densities were calculated at each time step of our simulation. Since the molecular collisions are not elastic, an inelastic energy loss of 30% was assumed for ion collisions with H_2O and OH due to electronic, rotational and vibration energy transfer, based on a separate molecular-dynamics calculation (Min Liu, Univ. of Virginia, private communication, 2001).

[10] Comparing to simpler non-collisional models [*Jurac et al.*, 2001b; *Richardson et al.*, 1998; *Ip*, 1997], we find that the momentum transfer, especially between fast O^+ ions and neutrals, produces a large inflation of the neutral cloud around the source region [*Smyth and Marconi*, 1993; *Decker and Cheng*, 1994]. If a close collision with a heavy ion (O^+, OH^+, H_2O^+) occurs, a neutral can be kicked out of Saturn's magnetosphere. More frequently, the collisions are glancing blows where only part of the collisional energy is transferred to the neutral, and the neutrals end up in more eccentric orbits with a higher likelihood of intersecting and being absorbed by the main rings.

[11] Figure 1 compares observed OH brightnesses in the equatorial plane (Figure 1a) and off the plane (Figure 1b) with model values (lines), assuming that the neutral cloud is a steady-state feature. The model values show a reasonable agreement with data over four years of observation, suggesting relatively constant OH densities over that period. We find that both collisional and dissociative momentum transfer are crucial for understanding the neutral cloud morphology. The collisional cross-section, smaller for faster moving particles, results in non-Maxwellian speed distributions with extended tails. Such a tail is apparent in Figure

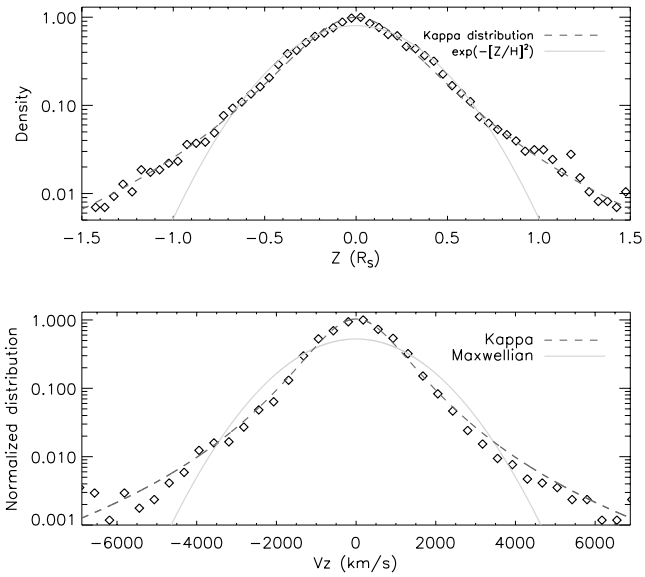

Figure 2. (a) The vertical density distribution of the OH cloud near Enceladus (3.5–4.5 R_S). Diamonds represent model densities normalized to the density in the equatorial plane. The densities are poorly described by the commonly assumed Gaussian scale height (solid line): $n(Z) = \exp(-(Z/H)^2)$, where *n* is the density, H = 0.37 is the scale height, and *Z* is the distance from the equatorial plane. The 1-D Kappa distribution with kappa-index k = 1.9 provides a good fit (dashed line). (b) Same for the V_z component of the OH velocity distribution but with k = 2.0.

2a, which shows that the vertical density profile obtained from our model is poorly described by the commonly assumed Gaussian scale height. Likewise, the velocity distribution exhibits a non-Maxwellian tail, indicating the absence of thermal equilibrium (Figure 2b). Both the density profile and the velocity distribution are well fit by the long-tailed Kappa distribution [*Vasyliūnas*, 1968] that characterizes many non-linear processes. Faster neutrals composing these fat-tails are less likely to cool down collisionally due to the smaller collisional cross sections at higher energies; their lifetime is further prolonged since these neutrals spend substantial portions of their orbits in the low-density high-latitude regions.

[12] Table 2 shows model OH densities near major satellites and the estimated source contributions that provide good agreement with the data. Rhea's contribution is poorly determined since the only observation from near its orbit had a large uncertainty. The model indicates that about 80% of the water comes from the Enceladus/E-ring region. A total H_2O source rate of $3.75 \cdot 10^{27}$ H_2O/s is required to maintain the observed neutral densities, almost three times the previous estimate of $1.4 \cdot 10^{27}$ H_2O/s [*Richardson et al.*, 1998]. Figure 3 shows the OH density profile derived from the model. The OH density peaks at Enceladus' orbit, but a significant portion of OH is contained inside 4 R_S. Beyond ~3 R_S collisions with corotating ions play a dominant role in depleting equatorial OH densities and inflating the cloud.

[13] Remarkably, the Mimas region appears to produce about 10 times more H_2O than Tethys or Dione, and the Enceladus region about 50 times more. This is the case in spite of the fact that Tethys and Dione are much larger

Table 2. Average OH Densities Derived From the Model, Moon's Distances, Radii, Surface Areas and Source Contributions as a Percentage of a Total Source Rate of $3.75 \cdot 10^{27}$ H_2O/s

Source region	OH cm^{-3}	Dist. R_S	Radius km	Surface Area 10^6 km^2	Source %
Mimas/G-ring/ F-ring ?	700	3.08	197	0.49	14
Enceladus/ E-ring	1000	3.95	250	0.79 E-ring: 0.8–3.2	83
Tethys	250	4.89	524	3.5	1.5
Dione	100	6.26	559	3.9	1.5
Rhea	10	8.74	764	7.3	< 1?

The spatial overlap between the E-ring and Enceladus, and also between Mimas and the G-ring, makes it hard to differentiate satellite from ring sources; we estimate their combined contribution assuming a satellite source. Unlike the surface area of the moons, the surface area of the rings is often uncertain since it can be only inferred indirectly: for the E ring lower and upper [*Juhasz and Horanyi*, 2002] limits are estimated. Dust clouds composed from tiny grains surrounding moons [*Krivov and Banaszkiewicz*, 2001] could enhance the effective surface area.

targets than Mimas and Enceladus for micrometeorites, grains or energetic ions, and therefore should provide more water. Thus, significantly larger surface areas than presently estimated would be needed near Enceladus and Mimas for any of these H_2O production mechanisms to account for the observed OH densities.

4. Implications

[14] Our model suggests that more than 80% of the total water vapor comes from Enceladus' orbital distance. The water source rate required to maintain the OH cloud corresponds to 112 kg/s, of which 93 kg/s must be coming from Enceladus orbital distance. Could E-ring particles originating from and later reimpacting Enceladus in a self-sustained fashion provide the necessary amount of water? Hypervelocity impact experiments show that a small grain

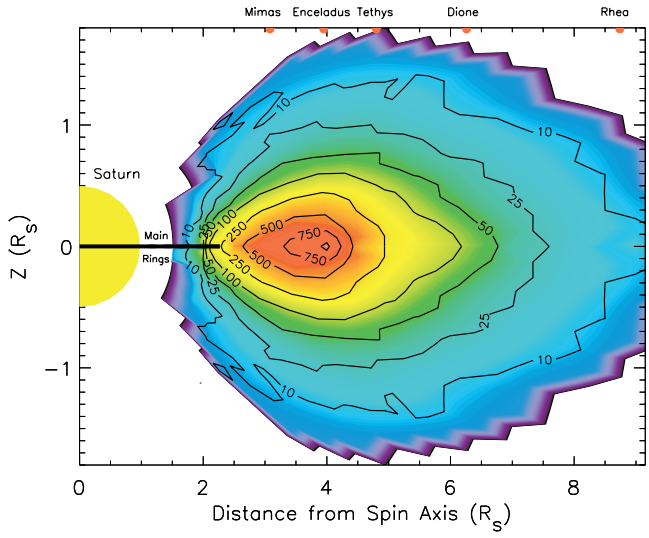

Figure 3. Cross section through Saturn's inner magnetosphere with OH density contours. Radial distances of major moons (red) are indicated on the X-axis, while the solid line represents the main rings. The sharp edges of the density contours (particularly the 500 and 750 cm^{-3} contours) between 4 and 5 R_S suggest the presence of a source close to Enceladus' orbit.

colliding with icy surface can produce a large quantity of solid ejecta, while a fraction of the impact energy is consumed in vaporization [*Erichorn and Grün*, 1993]. *Ip* [1997] estimated that if 60% of total dust particle population reimpacts Enceladus, $3.7 \cdot 10^{26}$ H_2O/s or 11 kg/s is produced. Even this optimistic scenario is almost an order of magnitude short of the H_2O needed to maintain the OH cloud. Unless the grain vaporization efficiency is seriously underestimated, more debris/grains residing around Enceladus would be needed to bring the Hamilton and Burns self-sustaining model into agreement with our source rate.

[15] *Paranicas and Cheng* [1997] inferred an absorbing surface area of unknown origin from the Voyager 2 plasma data. They estimated that a huge surface, 25 times larger than Enceladus' surface area, would be needed 30° behind Enceladus to account for the observed plasma microsignature. *Jurac et al.* [2001b] suggested that the disruption of a moonlet, which was a companion of Enceladus, produced debris near the Lagrangian L_5 point. The continued orbital collisions between debris could produce the observed bright arcs [*Roddier et al.*, 1998; *Barbara and Esposito*, 2002] and also generate a large surface area. In this picture the E-ring is not self-sustaining, but produced by such orbital collisions between the icy objects residing near Enceladus' Lagrangian points [*Roddier et al.*, 1998; *Jurac et al.*, 2001b].

[16] Interestingly, we find that a substantial amount of H_2O, 14%, originates from the vicinity of the tiny moon Mimas (3.08 R_S). Bright arcs, possibly also caused by collisions between moonlets [*Barbara and Esposito*, 2002], have recently been identified [*Poulet et al.*, 2000] in the neighboring F-ring (2.32 R_S), providing another potential link between orbital collisions and the source of water. Here we suggest that debris with radii ranging from micrometers to hundreds of meters collide and are further fragmented, producing E-ring grains and water vapor in the process. After becoming electrically charged, the tiniest fragments, sub-micron grains, are small enough to be substantially accelerated by the corotating magnetic field. Orbital simulations show that these grains do not drift substantially from their radial birthplaces [*Horanyi et al.*, 1992; *Dikarev*, 1999], but move faster than the larger fragments and moons, frequently impacting their trailing sides. Therefore, grains produced along Enceladus' orbit would impact the trailing sides of both Enceladus and any debris near the Lagrange points. A steady stream of water vapor can be then produced by grain sputtering and impact evaporation. A steady source is needed because HST measurements over four years suggest that the average neutral densities are relatively constant. Since the OH lifetime is about 3 months [*Richardson et al*, 1998], the cloud must be replenished on a shorter time-scale. The trailing side of Enceladus was recently found to display a bluish spectrum similar to that of the E-ring grains, and also to be substantially brighter than its leading side [*Momary et al.*, 2000], suggesting fresh deposits of E-ring material on the trailing side of the moon [*Showalter et al.*, 1991].

[17] **Acknowledgments.** S. J. wants to thank D. Shemansky for helpful suggestions. This work was supported by NASA Planetary Atmospheres grant NAGW 5-6129 to MIT and NASA Planetary Geology and Geophysics grant to UVA. The work at Tel Aviv University and Max-Planck-Institut für Aeronomie was supported in part by the German-Israeli foundation for Scientific Research and Development under grant I-562-242.07/97.

References

Barbara, J. M., and L. W. Esposito, Moonlet Collisions and the effects of tidally modified accretion in Saturn's F ring, submitted to *Icarus*, 2002.
Decker, R. B., and A. F. Cheng, A model of Triton's role in Neptune's magnetosphere, *J. Geophys. Res.*, *99*, 19,027–19,045, 1994.
Dikarev, V. V., Dynamics of particles in Saturn's E ring: Effects of charge variations and the plasma drag force, *Astron. Astrophys.*, *346*, 1011–1019, 1999.
Eckstein, W., in *Computer Simulation of Ion-Solid Interactions*, (Springer, Berlin), 40–99, 1991.
Eichhorn, G., and E. Grün, High-velocity impacts of dust particles in low-temperature water ice, *Planet. Space Sci.*, *41*, 429–433, 1993.
Hall, D. T., P. D. Feldman, J. B. Holberg, and M. A. McGrath, Flourescent hydroxyl emissions from Saturn's ring atmosphere, *Science*, *272*, 516–518, 1996.
Hamilton, D. P., and J. A. Burns, OH in Saturn's rings, *Nature*, *365*, 498, 1993.
Hamilton, D. P., and J. A. Burns, Origin of Saturn's E ring: Self sustained, naturally, *Science*, *264*, 550–553, 1994.
Horanyi, M., J. A. Burns, and D. P. Hamilton, The dynamics of Saturn's E-Ring particles, *Icarus*, *97*, 248–259, 1992.
Ip, W.-H., On the neutral cloud distribution in the Saturnian Magnetosphere, *Icarus*, *126*, 42–57, 1997.
Johnson, R. E., et al., The neutral cloud and heavy ion inner torus at Saturn, *Icarus*, *77*, 311–329, 1989.
Johnson, R. E., Rough stuff at Saturn, *Nature*, *363*, 300–301, 1993.
Juhasz, A., and M. Horanyi, Saturn's E ring: A dynamical approach, *J. Geophys. Res.*, in press, 2002.
Jurac, S., R. A. Baragiola, R. E. Johnson, and E. C. Sittler, Charging of ice grains by low energy plasmas: Application to Saturn's E ring, *J. Geophys. Res.*, *100*, 14,821–14,831, 1995.
Jurac, S., R. E. Johnson, J. D. Richardson, and C. Paranicas, Satellite sputtering in Saturn's magnetosphere, *Planet. Space Sci.*, *49*, 319–326, 2001a.
Jurac, S., R. E. Johnson, and J. D. Richardson, Saturn's E ring and production of the neutral torus, *Icarus*, *149*, 384–396, 2001b.
Krivov, A. V., and M. Banaszkiewicz, Unusual origin, evolution and fate of icy ejecta from Hyperion, *Planet. Space Sci.*, *49*, 1265–1279, 2001.
Momary, T. W., et al., The Saturnian satellites in the near-infrared: Absolute photometry at ring plane crossing, *Icarus*, *148*, 397–406, 2000.
Nicholson, P. D., et al., Observations of Saturn's ring-plane crossings in August and November 1995, *Science*, *272*, 509–515, 1996.
Paranicas, C., and A. F. Cheng, A model of satellite microsignatures for Saturn, *Icarus*, *125*, 380–396, 1997.
Pospieszalska, M. K., and R. E. Johnson, Micrometeorite erosion of the main rings as a source of plasma in the inner saturnian plasma torus, *Icarus*, *93*, 45–52, 1991.
Poulet, F., et al., Saturn's ring-plane crossings of August and November 1995: A model for the new F-ring objects, *Icarus*, *144*, 135–148, 2000.
Richardson, J. D., A. Eviatar, M. A. McGrath, and V. M. Vasyliunas, OH in Saturn's magnetosphere: Observations and implications, *J. Geophys. Res.*, *103*, 20,245–20,255, 1998.
Richardson, J. D., and E. C. Sittler Jr., A plasma density model for Saturn based on Voyager observations, *J. Geophys. Res.*, *95*, 12,019–12,031, 1990.
Richardson, J. D., Thermal plasma and neutral gas in Saturn's Magnetosphere, *Rev. Geophys.*, *36*, 501–524, 1998.
Roddier, C., F. Roddier, J. E. Graves, and M. J. Northcott, Discovery of an arc of particles near Enceladus's orbit: A possible key to the origin of the E ring, *Icarus*, *136*, 50–59, 1998.
Shemansky, D. E., P. Matherson, D. T. Hall, and T. M. Tripp, Detection of the hydroxyl radical in the Saturn's magnetosphere, *Nature*, *363*, 329–332, 1993.
Showalter, M. R., J. N. Cuzzi, and S. L. Larson, Structure and particle properties of Saturn's E ring, *Icarus*, *94*, 451–473, 1991.
Smyth, W. H., and M. L. Marconi, The nature of the hydrogen tori of Titan and Triton, *Icarus*, *101*, 18–32, 1993.
Vasyliūnas, V. M., A survey of low-energy electrons in the evening sector of the magnetosphere with OGO 1 and OGO 3, *J. Geophys. Res.*, *73*, 2839–2884, 1968.

S. Jurac and J. D. Richardson, M.I.T. 37-635, Cambridge, Massachusetts 02139, USA.
M. A. McGrath, Space Telescope Science Institute, Baltimore, Maryland, USA.
R. E. Johnson, University of Virginia, Charlottesville, Virginia, USA.
V. M. Vasyliūnas, Max-Planck-Institut für Aeronomie, Katlenburg-Lindau, Germany.
A. Eviatar, Tel Aviv University, Ramat Aviv, Israel.